

Article

Reduction in Energy Consumption by Mitigation of Cultivation Resistance Due to the New Fallow Harrow Concept

Volodymyr Bulgakov¹, Volodymyr Nadykto² , Olga Orynych^{3,*}  and Simone Pascuzzi^{4,*} 

¹ Department of Mechanics, Faculty of Construction and Design, National University of Life and Environmental Sciences of Ukraine, 15, Heroyiv Oborony Str., UA 03041 Kyiv, Ukraine

² Department of Machine-Using in Agriculture, Dmytro Motorny Tavria State Agrotechnological University, 18^B, Khmelnytsky Ave., UA 72310 Melitopol, Zaporozhye Region, Ukraine

³ Department of Production Management, Faculty of Engineering Management, Bialystok University of Technology, Wiejska Str. 45A, 15-351 Bialystok, Poland

⁴ Department of Soil, Plant and Food Science, University of Bari Aldo Moro, Via Amendola 165/A, 70126 Bari, Italy

* Correspondence: o.orynych@pb.edu.pl (O.O.); simone.pascuzzi@uniba.it (S.P.)

Abstract: One of the best precursors for winter wheat is fallow. Its application aims to solve two important tasks: preserving and accumulating soil moisture and weed control. The authors of this paper have designed a new modular harrow for fallow tillage, which can work stably at a depth of 5–6 cm tillage while maintaining and even accumulating soil moisture. This article describes a method designed by the authors for a reasonable selection of the design parameters concerning the working devices mounted inside the new harrow, such as their length and working width, as well as the angles of vertical inclination (ϵ) and horizontal deviation (γ) of blades, depending on the accepted depth of the upper soil layer loosening. To reduce the soil tillage resistance of the harrowing unit resulting in a reduction in the tractor fuel consumption, the value of the inclination angle (ϵ) of its vertical blade should be chosen so that the corresponding change in the value of the deflection angle of the horizontal blade (γ) complies with the constrain of the product of tangents of these angles. Moreover, preference should be given to choosing the value of the angle ϵ with the subsequent determination of the angle γ value. It is demonstrated that proper use of the new type of harrow assures fuel savings and decreases carbon dioxide emissions even if fossil fuel alone is used. Additional reduction of CO₂ emission can be achieved when biofuels are used as a replacement for fossil ones.

Keywords: soil; amplitude; fallow; thermal diffusivity; vibration frequency



Citation: Bulgakov, V.; Nadykto, V.; Orynych, O.; Pascuzzi, S. Reduction in Energy Consumption by Mitigation of Cultivation Resistance Due to the New Fallow Harrow Concept. *Energies* **2022**, *15*, 8500. <https://doi.org/10.3390/en15228500>

Academic Editor: Attilio Converti

Received: 24 October 2022

Accepted: 11 November 2022

Published: 14 November 2022

Publisher's Note: MDPI stays neutral with regard to jurisdictional claims in published maps and institutional affiliations.



Copyright: © 2022 by the authors. Licensee MDPI, Basel, Switzerland. This article is an open access article distributed under the terms and conditions of the Creative Commons Attribution (CC BY) license (<https://creativecommons.org/licenses/by/4.0/>).

1. Introduction

In sustainable agriculture, leaving a fallow field is widely recognized as one of the best methods for preparing winter wheat [1,2]. Moreover, this technological method is particularly effective if implemented using retardants [3]. Specific studies over 8 years have found that the traditional WW–SF (winter wheat–summer fallow) system is more efficient over annual no-till crop rotations in terms of higher average profitability and less economic volatility [4].

Using fallow lands allows the solution of two tasks: (i) soil moisture preservation and accumulation; (ii) weed control [5,6]. Consequently, in soil and climatic conditions where there is enough moisture in the soil at the time of sowing winter wheat, and the weed control problem is solved, fallow is not needed [7–9]. This circumstance is especially relevant for conditions with a high soil infiltration capacity due to the mobility of Cu and Zn cations [10].

At the same time, under conditions of moisture deficiency, there is a critical need to delay the sowing of winter wheat, even if, according to experimental studies, this

almost always leads to a decrease (sometimes significant) in the yield of this agricultural crop [11–13].

However, despite the different purposes, both tasks mentioned above for using fallow are currently solved through the systematic destruction of the upper soil layer capillaries. As a result, moisture evaporation decreases and weeds are destroyed [14]. At the same time, it was found that the refusal to cultivate fallow in summer due to the absence of weeds in the field leads to a significant loss of moisture from the soil [15]. Successful weed control must prevent soil clod formation, which impedes treatment [16,17].

Based on this, one-way discs and wide-blade cultivators are the implements most usually used in fallow lands with a tillage depth of at least 10 cm [18–20]. The disc harrows are used when trying to till the soil to a depth of 5 cm [21]. However, they still carry out moisture from the horizon of 0–5 cm to the field's surface. As a result, there are inevitably very significant soil moisture losses.

A conservation tillage system in arid zones has been proposed as a compromise [22,23], which provides for leaving more than 30% of the previous crop residues on the soil surface.

In general, the traditional technology of summer fallow, starting around August–September, may include eight or even more tillages [14], even if more intense moisture accumulation is expected in spring [24]. However, in reality, water conservation efficiency during fallow treatment is often less than 25% [25,26]. The rest of the moisture, according to the statements of these and other researchers [15], evaporates from the soil. Other studies highlighted that even to retain 25% of the falling moisture on the fallow fields, great efforts are required [27,28].

The reason for this result, in our opinion, is as follows. The working devices of the usually used tillage machines work stably only at a depth of at least 10 cm in the longitudinal–vertical plane. Unfortunately, the geometry of working devices is such that this soil layer is mixed and brought out from the depth to the day surface of the field. As a result, the soil of this layer (0–10 cm) undergoes further intensive drying.

Our studies have established that the highest intensity of moisture evaporation occurs in a soil layer up to 5–6 cm deep [29]. This result has found its practical application in a new ad hoc conceived harrow for fallow treatment, which provides for the systematic loosening of the soil to a depth of no more than 6 cm [30–32].

Due to the design originality of the tines of this new harrow for fallow treatment, there is a need for theoretical and experimental studies that would provide a rationale for the calculations and selection of their design parameters. The current general theoretical developments for solving such a problem are unsuitable. The main reason is that most of these theoretical studies' results consider the surface curvature of the soil-cultivating working devices. In contrast, in our new harrow, the working tines do not have any curved surface.

This work aims to substantiate the operative parameters of the new harrow for fallow treatment based on the results of theoretical and experimental studies. Assessing the operative parameters means reducing the tillage resistance force and then improving the energy saving due to lowering the tractor fuel consumption.

2. Materials and Methods

2.1. The New Harrow Machine

The authors conceived and built a harrow formed by modular units suitable for fallow land tillage. Each module unit of the harrow (Figure 1) consists of a steel reticular frame on which 20 tines (5 rows each with 4 tines) are mounted according to a zigzag pattern. Each tine is formed by an 8 mm thick vertical flat steel bar (spike tooth), to which end, a flat blade is welded with a working width of 80 mm. The front row tines of the modular unit are also equipped with a vertical blade to facilitate the shredding of plant residues, which could arise in the upper soil layer (up to 6 to 7 cm depth). Each harrow modular unit is connected by linking rods to a common supporting beam, which in turn is connected to the tractor.

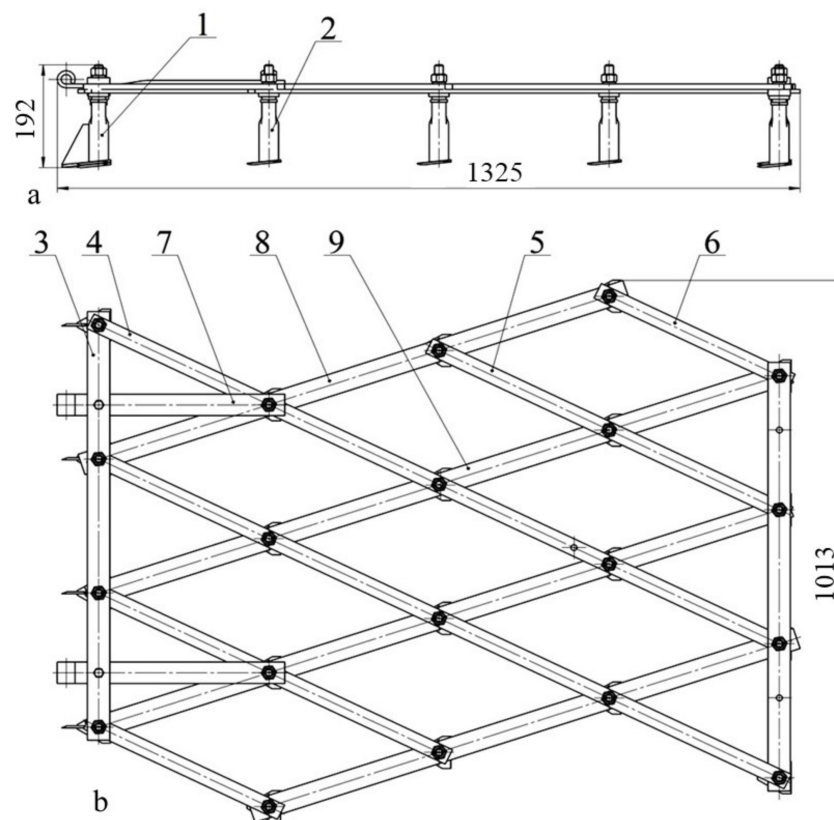


Figure 1. View of the harrowing modular unit equipped with flat-cutting devices: (a)—side view; (b)—view from above: 1—front tine; 2—tine; 3—crossbar; 4, 5, 6, 8, and 9—rods forming the reticular frame; and 7—linking rods (measures in mm).

2.2. Theoretical Considerations

The soil tillage resistance force P_v , which acts on the vertical blade of the tine (Figure 2), can be assessed by the following equation:

$$P_v = \frac{q_s \cdot b}{\cos \epsilon}, \quad (1)$$

where q_s is the specific soil tillage resistance due to the interaction of the soil–harrow tine, $\text{N} \cdot \text{m}^{-1}$; b is the height of the vertical cutting blade, m; and ϵ is the tine blade's inclination angle to the vertical, grad.

The horizontal blade mounted on the blade is deflected in the horizontal plane by the angle γ and is under the influence of two soil tillage resistance forces P_h , each of which can be evaluated as follows:

$$P_h = q_s \cdot L_o, \quad (2)$$

where L_o is the length of one blade's side (Figure 2), m.

As follows from the analysis of Figure 2:

$$L_o \cdot \cos \gamma = b \cdot \tan \epsilon, \quad (3)$$

From which it follows:

$$L_o = \frac{b \cdot \tan \epsilon}{\cos \gamma}. \quad (4)$$

Considering Equations (2) and (4) will have the following form:

$$P_h = q_s \cdot b \cdot \frac{\tan \epsilon}{\cos \gamma}. \quad (5)$$

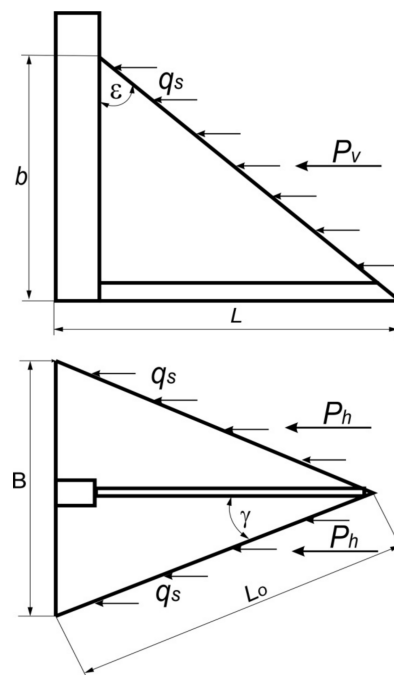


Figure 2. Scheme of forces acting on the tine for fallow treatment.

The total soil tillage resistance force on a given tine (P_o) at a tillage depth h is equal to the following equation:

$$P_o = P_v + 2P_h. \quad (6)$$

Taking the value of the parameter b (see Figure 2) equal to the tillage depth h and substituting formulas (1), as well as (5) into Equation (6), after transformations, the following can be obtained:

$$P_o = \frac{q_s \cdot h}{\cos \epsilon} \cdot \left(1 + 2 \cdot \frac{\sin \epsilon}{\cos \gamma} \right). \quad (7)$$

In addition to the values of the angles γ and ϵ , the main parameters of the considered tine include dimensions B and L (Figure 2). The following equations are valid for their calculation:

$$L = h \cdot \tan \epsilon; \quad (8)$$

$$B = 2h \cdot \tan \epsilon \cdot \tan \gamma. \quad (9)$$

As the results of preliminary field experimental studies have shown, these working devices can work stably at a tillage depth of 5–6 cm if the value of parameter B does not exceed 0.10 m. At $B = 0.06$ m, a minimum overlap (1 cm) of tillage zones between adjacent tracks laid by the harrow tines is provided. From this, it follows that:

$$0.06 \leq B = 2h \cdot \tan \epsilon \cdot \tan \gamma \leq 0.10. \quad (10)$$

At $h = 5$ cm, the condition determined by Equation (10) takes the following final form:

$$0.6 \leq \tan \epsilon \cdot \tan \gamma \leq 1. \quad (11)$$

The analytical Equations (7)–(11), which are based on the results of theoretical studies, make it possible to determine a scientifically substantiated selection of the design parameters of the tines of the conceived harrow for fallow lands tillage. The criterion determining their rational values is the minimum soil tillage resistance force P_o acting on the tine at a given fallow land tillage depth (h). The minimum soil tillage resistance allows energy savings by reducing the fuel consumption of the tractor attached to the new harrow.

2.3. Experimental Methodology

The resulting Equation (7) can be used for calculations of the real value of the specific soil tillage resistance q_s applied by the soil on the harrow tine during activation. This parameter has been experimentally assessed through fallow lands tillage carried out employing a harrowing experimental aggregate formed by: (i) MTZ-82 wheeled tractor of 60 kW; and (ii) the harrow conceived and built by us, which was composed of 9 modular units (Figure 3).



Figure 3. Tractor with harrow for treatment fallow.

Experimental studies were executed under field conditions characterized by the following geographic data: 46°50'56" north latitude, 35°21'55" east longitude, altitude: 37 m. The soil type was dark chestnut chernozem, and the granulometric composition was heavy loamy since the content of physical clay was 46–48%. Furthermore, the humus content was in the range of 2.8–3.6%, and the reaction of the soil solution was close to neutral.

The soil moisture content in the layer 0–5 cm was measured by an ad hoc device designed by us (Figure 4), whose working principle was based on the changes in the soil dielectric permeability depending on its moisture content. A piston was mounted on the device's top cover to compact the soil, whereas the electronic recording part was located on the lower cover of the device. The soil sample was placed on the device's glass and compacted by the piston. The value of its humidity (%) was fixed on the device. The measurement error of this device did not exceed 1%. Crossing the soil diagonally, the moisture content was measured on soil samples taken every 3 m. Globally, 100 moisture content measurements were carried out and the average value was assumed for subsequent numerical processing.

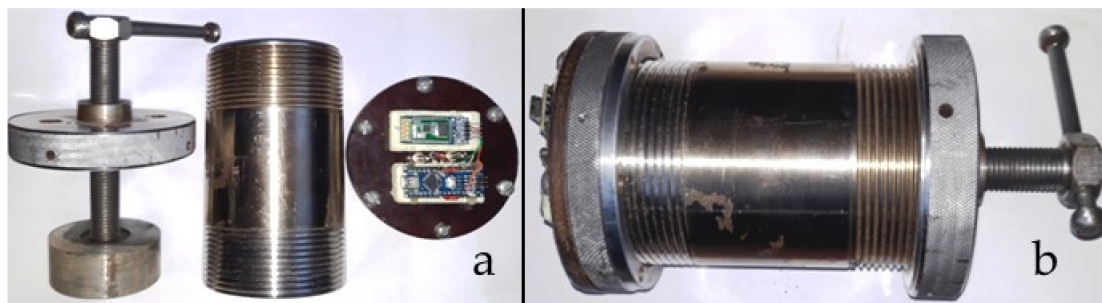


Figure 4. Soil humidity measuring device: (a)—constituent elements; (b)—general form.

The soil bulk density was evaluated by means of a device equipped with a 28.35 cm³ cylinder and a scale that directly displays the soil density value in g cm⁻³ [33]. The soil bulk density was measured in the soil layer of 0–5 cm in 10 repetitions.

The tillage depth performed by the developed harrow was measured at the two ends and the center of the implement. Two repetitions were considered. The measurement

step of the depth was 0.2 m, and 300 evaluations were performed in each repetition. A measuring device built by us was used, essentially based on an ultrasonic sensor HC-SR04 (Kuangshun Electronic, Shenzhen, China) connected via USB cable to the Arduino Mega 2560 microcontroller platform (Figure 5). The main technical features of the HC-SR04 sensor were as follows: measuring range from 0.02 to 4 m; working frequency 40 Hz. The error in measuring the tillage depth with this device did not exceed 0.5 cm.



Figure 5. Kit for measuring tillage depth.

The soil tillage resistance coefficient q_s was evaluated as follows. The soil tillage resistance force was assessed through foil tensoresistors, having a nominal value of 200 Ohm and constant voltage of 12 V, which were glued on the linking rods of three modular units of the harrow implement (the two outside ones and the middle one, respectively). The sensor signal was fed to the computer through an analog-to-digital converter (ADC, Figure 6). During the test, the soil tillage resistance force pertinent to each of the three considered harrow units was recorded for 60 s.

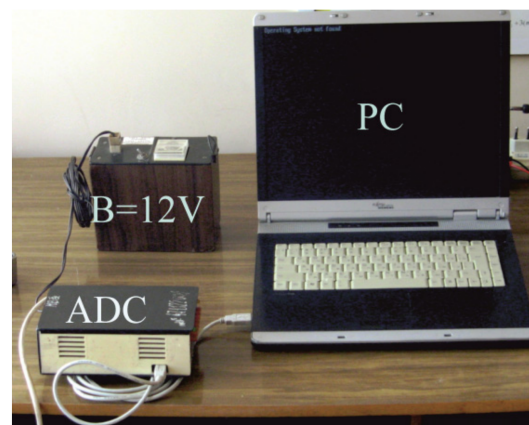


Figure 6. Measuring and recording complex.

The obtained soil tillage resistance force values were processed and the average value was calculated. Considering that the working width of each harrow unit was approximately 1 m (Figure 1), this calculated average value was taken equal to the soil tillage resistance per unit length R_a ($\text{N}\cdot\text{m}^{-1}$) of the harrow implement. Finally, considering that each harrow unit included 20 tines, the specific soil tillage resistance q_s corresponding to each tine was calculated as follows:

$$q_s = \frac{R_a}{20}. \quad (12)$$

The value of the q_s parameter established in this way was used for theoretical studies using Equations (7)–(11).

Before conducting research, the field was divided into sets with a length of $L_a = 250$ m each. The time (t_a) for the harrow implement to pass through the set in two repetitions

was recorded using an FS-8200 electronic stopwatch (FLOTT, Shanghai, China) with a measurement accuracy of up to 0.1 s. The speed of the machine–tractor unit movement was calculated with the formula: $V = L_a \cdot (t_a)^{-1}$.

3. Results and Discussion

The experimental fallow land tillage aimed at assessing the q_s value was carried out with the following soil conditions: (i) moisture content in the 0–5 cm layer, 18.3%; (ii) bulk density, 1220.0 kg m⁻³. The harrowing experimental aggregate moved at a speed of 2.2 m·s⁻¹. With a confidence level of 95%, the confidence interval for the harrowing depth tillage of the fallow field was 6.1 ± 0.2 cm. The obtained average value of the q_s parameter, which was subsequently adopted for theoretical studies, was 230 N·m⁻¹.

An analysis of Equation (7) shows that the value of the total soil tillage resistance force (P_o) changes linearly with an increase in the parameters q_s and h , which is quite logical. In principle, the influence of the angle γ on this force is also understandable. First, an increase in its value leads, as follows from Equation (7), to a decrease in the $\cos\gamma$ function and hence to an increase in the value of P_o . Secondly, an increase in the value of the angle γ according to Equation (9) causes an increase in the design width of the working device blade (B , Figure 2), and hence an increase in the value of the P_o force. Another thing is that the functional dependence $P_o = f(\gamma)$ is non-linear and therefore is of interest for study.

The effect of changing the value of the angle ϵ on the soil tillage resistance force P_o magnitude is very problematic to assess visually. A graphical interpretation of this process is needed. Moreover, the change in the parameter ϵ is organically related to the corresponding change in the value of the angle γ . The nature of this connection is established by analytical Equations (10) and (11).

Analysis of the results obtained using the analytical Equation (7), considering the requirement (11), showed that an increase in the value of the angle ϵ leads to a corresponding increase in the total soil tillage resistance P_o value (Figure 7).

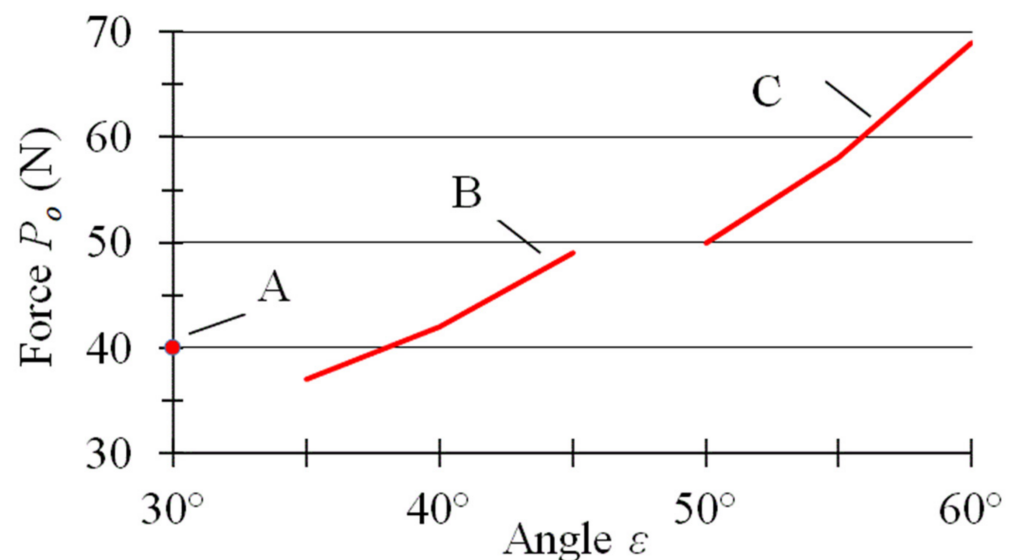


Figure 7. The dependence on the soil tillage resistance P_o on the angle ϵ for the following values of the angle γ : 60° (point A); 45° (curve B); and 30° (curve C).

Moreover, the greater this growth, the smaller the value of the angle γ . If γ is equal to 30° (curve C, Figure 7), the angle ϵ changes within 50–60° and the level of P_o force growth was the highest: it increased from 50 to 70 N, i.e., by 40%. At $\gamma = 45^\circ$, the angle ϵ changes in a range of 10°, but the level of P_o force increase is less and equals 30% (curve B, Figure 7).

The design variant of the working device corresponding to $\gamma = 60^\circ$ requires a singular remark. In this case, the condition in Equation (11) is satisfied only for one angle ϵ value equal to 30° and the P_o force assumes a fixed value of 40 N (point A, Figure 7).

In general, the following pattern of change in the functional dependence $P_o = f(\epsilon)$ takes place: to reduce the total soil tillage resistance force P_o , the decrease in the value of the angle ϵ must be accompanied by a corresponding increase in the value of the angle γ , so that condition (11) is met. The functional dependence $P_o = f(\gamma)$ concerning the dependence $P_o = f(\epsilon)$ is as follows. For each specific value of the angle ϵ , the value of the soil tillage resistance P_o is directly proportional to the change in the value of the angle γ . The exception is the design variant of the considered harrow working device at $\epsilon = 60^\circ$. In this case, condition (11) is satisfied only for one value of the angle γ , which is equal to 30° . The soil tillage resistance P_o takes a fixed value of 69 N (point A, Figure 8).

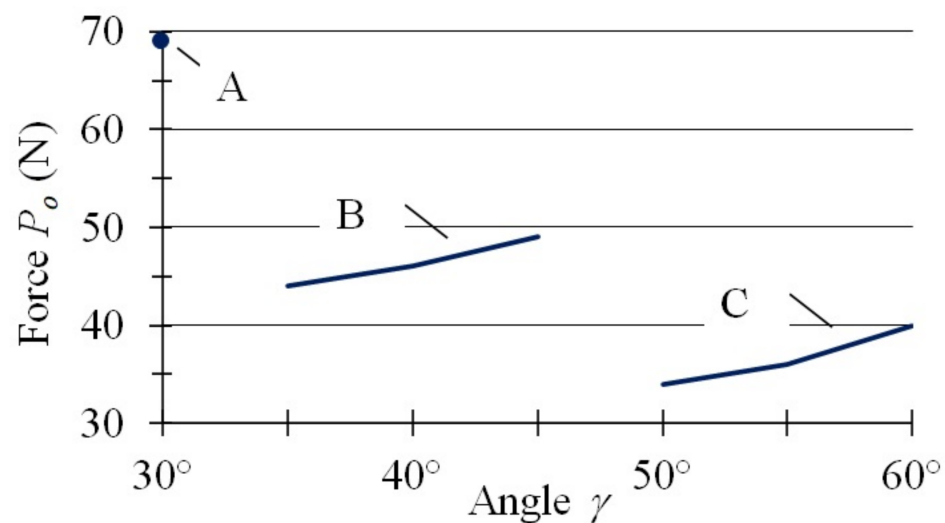


Figure 8. The dependence on the soil tillage resistance P_o on the angle γ for different values of the angle ϵ : 60° (point A); 45° (curve B); and 30° (curve C).

As a result, if the value of the angle γ is increased at a certain constant value of the angle ϵ , which does not exceed 60° , then the value of the soil tillage resistance force P_o also increases (see Figure 8). The only peculiarity is that the intensity of such growth (that is, the rate of the indicated force change) is much lower than for the functional dependence $P_o = f(\epsilon)$. This result can be more clearly demonstrated by considering the following derivatives:

$$\frac{\partial P_o}{\partial \epsilon} = 2q_s \cdot h \cdot \left(\frac{\tan^2 \epsilon + 1}{\cos \gamma} + \frac{\sin \epsilon}{2 \cos^2 \epsilon} \right). \quad (13)$$

and

$$\frac{\partial P_o}{\partial \gamma} = 2q_s \cdot h \cdot \tan \epsilon \cdot \frac{\sin \gamma}{\cos^2 \gamma}. \quad (14)$$

The analysis of Equations (13) and (14) once again confirm that the increase in the soil tillage resistance force P_o on the working device by making the angle ϵ large (zones A₁, B₁, and C₁; Figure 9) is 2.5–3.5 times higher than the one produced by similar changes in the angle γ (zones A, B, and C; Figure 9). These characteristics should be considered when choosing the working device parameters for fallow treatment.

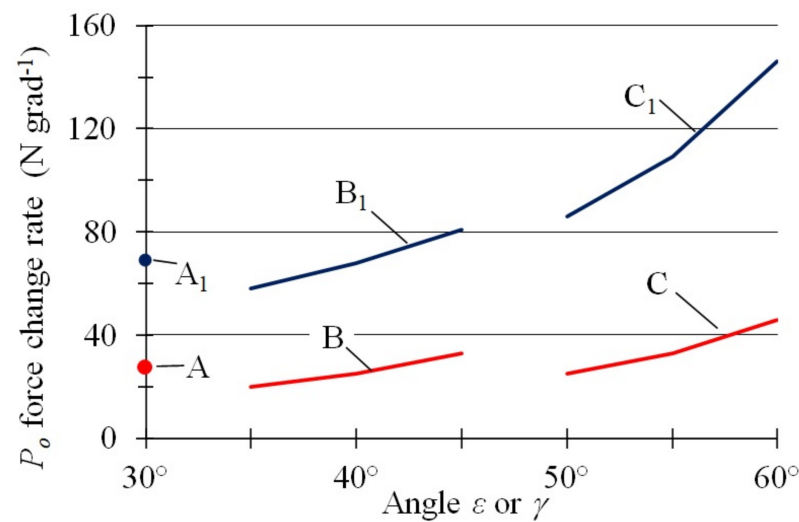


Figure 9. Dynamics of change $\partial P_o \cdot (\partial \gamma)^{-1}$ (—) and $\partial P_o \cdot (\partial \epsilon)^{-1}$ (—) depending on the angles *epsilon* and γ : $\gamma = 60^\circ$ (point A); *epsilon* = 60° (point A_1); $\gamma = 45^\circ$ (curve B); $\epsilon = 45^\circ$ (curve B_1); $\gamma = 30^\circ$ (curve C); and *epsilon* = 30° (curve C_1).

From the above analysis, it follows that when reducing total soil tillage resistance force P_o of the harrow working device, preference should be given to choosing the value of the angle ϵ , followed by determining the value of the angle γ within the performing condition (11). The basis for such a statement is a more intense change in the value of the resistance force P_o with an increase or, vice versa, a decrease in the value of the angle ϵ compared with a similar change in the angle γ .

As follows from Equations (8) and (9), the angles ϵ and γ , together with the value of the tillage depth (h), uniquely determine the design parameters as the length (L) and the width (B) of the working device for loosening fallow. According to Equation (8), the parameter L is formally independent of the value of the angle γ . This is not true due to the presence of the condition in Equation (11). If, for example, the angle ϵ varies within 50 – 60° (curve C, Figure 10), then to meet the condition of Equation (11), the angle γ must have a random value and not a specific one, equal in this case to 30° . The value of the parameter L changes in this case within 6–9 cm.

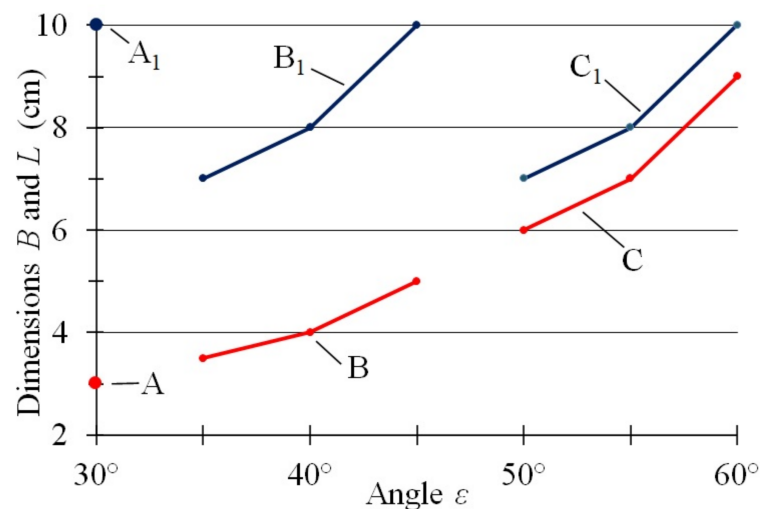


Figure 10. Dependence of parameters B (—) and L (—) of the harrow tine on the value of the angle *epsilon* for different values of the angle γ : 60° (point A, A_1); 45° (curve B and curve B_1); and 30° (curve C and curve C_1).

The selection of the angle ϵ value within 35–45° is possible only if the value of the angle γ is 45° and, accordingly, the value of the parameter L is in a narrower range, that is 3.5–5.0 cm (curve B, Figure 10). If the selected value of the angle ϵ is equal to 30°, then to meet the condition of Equation (11), the value of the angle γ must be equal to 60°, and the length of the working device for fallow soil treatment should be 3 cm (point A, Figure 10).

In agreement with Equation (9), the width of the harrow working device for fallow soil treatment (parameter B) depends on the values of both angles. Therefore, if the angle ϵ varies within 50–60° (curve C_1), the angle γ is equal to 30°, and the parameter B can take values from 7 to 10 cm.

If the angle ϵ changes from 35 to 45° (curve B_1 , Figure 10), the angle γ should be 45°, but the range of parameter B values remain the same: 7–10 cm. This result has the following explanation. When the values of the angle ϵ decrease from 50–60° to 35–45°, the values of the angle γ increase from 30 to 45°. Since the parameter B depends, as follows from Equation (9), on the product of the tangents of these angles, the range of its values remains unchanged. In other words, according to the condition of Equation (11), the value of the working device width for fallow treatment (i.e., B parameter) is invariant concerning the product $\tan \epsilon = \tan \gamma$. For the specific case, $\epsilon = 30^\circ$ and $\gamma = 60^\circ$, the parameter B has a single fixed value equal to 10 cm (point A_1 , Figure 10).

4. Conclusions

Referring to a harrow of a new concept useful in sustainable agriculture for fallow lands tillage, a method was studied to determine a reasonable selection of the design parameters of the working devices mounted inside this implement, such as their length (L) and working width (B), as well as the angle of the vertical inclination (ϵ) and the angle of the horizontal deviation (γ) of the blades, depending on the accepted loosening soil depth (h).

The selection of the inclination angle of the vertical blade (ϵ) should be accompanied by a corresponding change in the deviation angle of the horizontal blade (γ), so that the condition of Equation (11) associated with the product of the tangents of these angles is met.

To reduce the resistance force of the fallow harrow working device and then obtain fuel saving of the tractor linked to the harrow of the new concept, preference should be given to choosing the value of the angle ϵ , followed by determining the value of the angle γ within the limits of the performing condition of Equation (11). The basis for such a statement is a more intense change in the value of the resistance force with an increase or, vice versa, a decrease in the value of the angle ϵ compared with a similar change in the angle γ .

Due to the action of the condition determined by the analytical Equation (11), the device working width for fallow treatment (i.e., parameter B) is invariant concerning the product of the tangents of the angles ϵ and γ .

It has been shown that the correct use of the new type of harrow saves fuel and reduces carbon dioxide emissions even when using only fossil fuel. An additional reduction in CO₂ emissions can be achieved by using biofuels as a substitute for fossil fuels.

Author Contributions: Conceptualization and methodology, V.B., S.P., V.N. and O.O.; formal analysis, investigation, and data curation, V.B., S.P., O.O. and V.N.; writing—original draft preparation, V.B., S.P., V.N. and O.O.; writing—review and editing, V.B., S.P., O.O. and V.N.; supervision, V.B., S.P., V.N. and O.O. All authors have read and agreed to the published version of the manuscript.

Funding: Financing under the project WZ/WIZ-INZ/4/2022 research conducted in part during cooperation stays in Lithuania, 2021, 2022; Slovakia, 2021; and České Budějovice, 2022; and an internship at the Lublin University of Technology, 2021, 2022.

Institutional Review Board Statement: Not applicable.

Informed Consent Statement: Not applicable.

Acknowledgments: O. Orynych expresses gratitude for the financial contribution from Bialystok University of Technology No. WZ/WIZ-INZ/4/2022.

Conflicts of Interest: The authors declare no conflict of interest.

References

1. Ghimire, R.; Ghimire, B.; Mesbah, A.O.; Sainju, U.M.; Idowu, O.J. Soil health response of cover crops in winter wheat-fallow system. *Agron. J.* **2019**, *111*, 2108–2115. [[CrossRef](#)]
2. Guerrieri, A.S.; Anifantis, A.S.; Santoro, F.; Pascuzzi, S. Study of a Large Square Baler with Innovative Technological Systems that Optimize the Baling Effectiveness. *Agriculture* **2019**, *9*, 86. [[CrossRef](#)]
3. Bogomazov, S.V.; Kochmin, A.G.; Tkachuk, O.A.; Pavlikova, E.V.; Sharunov, O.A. Effects of precursor and growth regulators on the productivity of winter wheat. *Bulg. J. Crop Sci.* **2017**, *54*, 29–34.
4. Schillinger, W.F.; Kennedy, A.C.; Young, D.L. Eight years of annual no-till cropping in Washington’s winter wheat-summer fallow region. *Agric. Ecosyst. Environ.* **2007**, *120*, 345–358. [[CrossRef](#)]
5. Hunt, J.R.; Browne, C.; McBeath, T.M.; Verburg, K.; Craig, S.; Whitbread, A.M. Summer fallow weed control and residue management impacts on winter crop yield through soil water and N accumulation in a winter-dominant, low rainfall region of southern Australia. *Crop Pasture Sci.* **2013**, *64*, 922–934. [[CrossRef](#)]
6. Kettler, T.A.; Lyon, D.J.; Doran, W.; Powers, W.L.; Stroup, W.W. Soil Quality Assessment after Weed-Control Tillage in a No-Till Wheat-Fallow Cropping System. *Soil Sci. Soc. Am. J.* **2000**, *64*, 339–346. [[CrossRef](#)]
7. Schillinger, W.F. Minimum and Delayed Conservation Tillage for Wheat-Fallow Farming. *Soil. Sci. Soc. Am. J.* **2001**, *65*, 1203–1209. [[CrossRef](#)]
8. Janosky, J.S.; Young, D.L.; Schillinger, W.F. Economics of Conservation Tillage in a Wheat-Fallow Rotation. *Agron. J.* **2002**, *94*, 527–531. [[CrossRef](#)]
9. Dahiya, R.; Ingwersen, J.; Streck, T. The effect of mulching and tillage on the water and temperature regimes of a loess soil: Experimental findings and modeling. *Soil Tillage Res.* **2007**, *96*, 52–63. [[CrossRef](#)]
10. Angelaki, A.; Dionysidis, A.; Sihag, P.; Golia, E.E. Assessment of Contamination Management Caused by Copper and Zinc Cations Leaching and Their Impact on the Hydraulic Properties of a Sandy and a Loamy Clay Soil. *Land* **2022**, *11*, 290. [[CrossRef](#)]
11. Donaldson, E.; Schillinger, W.F.; Dofing, S.M. Straw Production and Grain Yield Relationships in Winter Wheat. *Crop Sci.* **2001**, *41*, 100–106. [[CrossRef](#)]
12. Li, R.; Ma, J.; Sun, X.; Guo, X.; Zheng, L. Simulation of Soil Water and Heat Flow under Plastic Mulching and Different Ridge Patterns. *Agriculture* **2021**, *11*, 1099. [[CrossRef](#)]
13. Goncharov, V.M.; Shein, E.V. *Agrophysics*; Fenix: Rostov-na-Don, Russia, 2006; ISBN 978-5222077412. (In Russian)
14. Al-Mulla, Y.A.; Wu, J.Q.; Singh, P.; Flury, M.; Schillinger, W.F.; Huggins, D.R.; Stöckel, C.O. Soil water and temperature in chemical versus reduced-tillage fallow in a Mediterranean climate. *Appl. Eng. Agric.* **2009**, *25*, 45–54. [[CrossRef](#)]
15. Riar, D.S.; Ball, D.A.; Yenish, J.P.; Wuest, S.B.; Corp, M.K. Comparison of fallow tillage methods in the intermediate rainfall inland Pacific Northwest. *Agron. J.* **2010**, *102*, 1664–1673. [[CrossRef](#)]
16. Peruzzi, A.; Ginanni, M.; Fontanelli, M.; Raffaelli, M.; Bärberi, P. Innovative strategies for on-farm weed management in organic carrot. *Renew. Agric. Food Syst.* **2007**, *22*, 246–259. [[CrossRef](#)]
17. Peruzzi, A.; Martelloni, L.; Frascioni, C.; Fontanelli, M.; Pirchio, M.; Raffaelli, M. Machines for non-chemical intra-row weed control in narrow and wide-row crops: A review. *J. Agric. Eng.* **2017**, *48*, 57–70. [[CrossRef](#)]
18. Lindwall, C.W.; Anderson, D.T. Agronomic evaluation of minimum tillage systems for summer fallow in southern Alberta. *Can. J. Plant Sci.* **1981**, *61*, 247–253. [[CrossRef](#)]
19. Bulgakov, V.; Pascuzzi, S.; Ivanovs, S.; Nadykto, V.; Nowak, J. Kinematic discrepancy between driving wheels evaluated for a modular traction device. *Biosyst. Eng.* **2020**, *196*, 88–96. [[CrossRef](#)]
20. Pascuzzi, S.; Anifantis, A.S.; Santoro, F. The concept of a compact profile agricultural tractor suitable for use on specialised tree crops. *Agriculture* **2020**, *10*, 123. [[CrossRef](#)]
21. Schillinger, W.F.; Papendick, R.I. Tillage Mulch Depth Effects during Fallow on Wheat Production and Wind Erosion Control Factors. *Soil Sci. Soc. Am. J.* **1997**, *61*, 871–876. [[CrossRef](#)]
22. Schillinger, W.F.; Papendick, R.I.; Guy, S.O.; Rasmussen, P.E.; van Kessel, C. *Dryland Agriculture*, 2nd ed.; American Society of Agronomy: Madison, WI, USA; Crop Science Society of America: Madison, WI, USA; Soil Science Society of America: Madison, WI, USA, 2006; pp. 365–393.
23. Smith, E.G.; Peters, T.L.; Blackshaw, R.E.; Lindwall, C.W.; Larney, F.J. Economics of reduced tillage fallow-crop systems in the dark brown soil zone of Alberta. *Can. J. Soil Sci.* **1996**, *76*, 411–416. [[CrossRef](#)]
24. Chang, C.; Sommerfeldt, T.G.; Entz, T.; Stalker, D.R. Long-term soil moisture status in Southern Alberta. *Can. J. Soil Sci.* **1990**, *70*, 125–136. [[CrossRef](#)]
25. Lyon, D.J.; Baltensperger, D.D.; Blumenthal, J.M.; Burgener, P.; Harveson, R.M. Eliminating Summer Fallow Reduces Winter Wheat Yields, but Not Necessarily System Profitability. *Crop Sci.* **2004**, *44*, 855–860. [[CrossRef](#)]
26. Massee, T.W.; Cary, J.W.; Plains, G.; Desert, A. Potential for reducing evaporation during summer fallow. *J. Soil Water Conserv.* **1978**, *33*, 126–129.

27. Mielke, L.N.; Wilhelm, W.W.; Richards, K.A.; Fenster, C.R. Soil Physical Characteristics of Reduced Tillage in a Wheat-Fallow System. *Trans. Am. Soc. Agric. Eng.* **1984**, *27*, 1724–1728. [[CrossRef](#)]
28. Licht, M.A.; Al-Kaisi, M. Strip-tillage effect on seedbed soil temperature and other soil physical properties. *Soil Tillage Res.* **2005**, *80*, 233–249. [[CrossRef](#)]
29. Adamchuk, V.; Bulgakov, V.; Nadykto, V.; Ivanovs, S. Investigation of tillage depth of black fallow impact upon moisture evaporation intensity. *Eng. Rural. Dev.* **2020**, 377–383. [[CrossRef](#)]
30. Bulgakov, V.; Nadykto, V.; Kaminskiy, V.; Ruzhylo, Z.; Volskyi, V.; Olt, J. Experimental research into the effect operating speed on uniformity of cultivation depth during tillage in fallow field. *Agron. Res.* **2020**, *18*, 1962–1972. [[CrossRef](#)]
31. Bulgakov, V.; Ivanovs, S.; Nadykto, V.; Kaminskiy, V.; Shymko, L.; Kaletnik, H. Movement Stability of a Section of the Machine for Black Fallow Cultivation in a Longitudinal-Verticale Plane. *INMATEH Agric. Eng.* **2020**, *62*, 99–106. [[CrossRef](#)]
32. Orynych, O.A. *Influence of Tillage Technology on the Energy Efficiency of a Rapeseed Plantation*, *Procedia Engineering*; Elsevier: Amsterdam, The Netherlands, 2017; Volume 182, pp. 532–539. [[CrossRef](#)]
33. Nadykto, V.; Kyurchev, V.; Bulgakov, V.; Findura, P.; Karaiev, O. Influence of the plough with tekron moldboards and landsides on ploughing parameters. *Acta Technol. Agric.* **2020**, *1*, 40–45. [[CrossRef](#)]